Femtosecond pump–probe spectroscopy of graphene oxide in water

2014 J. Phys. D: Appl. Phys. 47 094008

IOP Publishing Journal of Physics D: Applied Physics
J. Phys. D: Appl. Phys. **47** (2014) 094008 (7pp) doi:10.1088/0022-3727/47/9/094008

Femtosecond pump–probe spectroscopy of graphene oxide in water

Jingzhi Shang[1], Lin Ma[1], Jiewei Li[1,2], Wei Ai[1,2], Ting Yu[1,3,4] and Gagik G Gurzadyan[1]

[1] Division of Physics and Applied Physics, School of Physical and Mathematical Sciences, Nanyang Technological University, Singapore 637371, Singapore
[2] Key Laboratory for Organic Electronics & Information Displays (KLOEID) and Institute of Advanced Materials (IAM), Nanjing University of Posts and Telecommunications, Nanjing 210046, People's Republic of China
[3] Department of Physics, Faculty of Science, National University of Singapore, Singapore 117542, Singapore
[4] Graphene Research Centre, National University of Singapore, 2 Science Drive 3, Singapore 117542, Singapore

E-mail: Gurzadyan@ntu.edu.sg and Yuting@ntu.edu.sg

Received 16 April 2013, revised 29 May 2013
Accepted for publication 18 June 2013
Published 12 February 2014

Abstract

Transient absorption properties of aqueous graphene oxide (GO) have been studied by use of femtosecond pump–probe spectroscopy. Excited state absorption and photobleaching are observed in the wide spectral range. The observed fast three lifetime components are attributed to the absorption of upper excited states and localized states, which is confirmed by both laser induced absorption and transmission kinetics. The longest time component is assigned to the lowest excited state of GO, which mainly originates from the sp2 domains. With the increase of the excitation power, two-quantum absorption occurs, which results in an additional rise-time component of the observed transients.

(Some figures may appear in colour only in the online journal)

1. Introduction

Graphene oxide (GO) and reduced graphene oxide (rGO) have attracted great attention due to promising applications [1–3], such as conducting thin films [4], supercapacitors composites [5], biosensing devices [6] and nonlinear optical materials [7]. Recently, more characteristics of GO and rGO have been revealed [8–10]. Investigation of optical properties of GO is very important for understanding the fundamentals of the structure and the electronic transitions. Previously, the broad visible fluorescence has been observed in GO prepared by various strategies, where the origin of fluorescence has also been discussed based on both steady-state [11–19] and time-resolved fluorescence measurements [15, 18–20]. Particularly, the carrier dynamics in rGO has been found to be dependent on the degree of oxygen reduction [18]. Meanwhile, the main absorption bands of GO have been found in the ultraviolet spectral region [13, 21]. Transient absorption measurements of GO have revealed the various carrier decay processes [22–25]. Zhao *et al* have reported three decay components of GO suspensions and attributed them to carrier-optical phonon scattering, carrier-acoustic phonon scattering and carrier interband recombination process [25]. Liu *et al* have observed the flipped carrier decay signal at the wavelength of 800 nm and proposed sp2 and sp3 domains contributing to the carrier relaxation differently, where sp2 and sp3 domains are responsible for the photobleaching and excited state absorption, respectively [23]. Ruzicka *et al* [24] and Zhao *et al* [25] have reported the carrier dynamics in rGO with strong oxygen reduction, where the decay constants are comparable with those from graphene. Moreover, Kaniyankandy *et al* have observed multi-exponential relaxation, where the long time constant (>400 ps) has been attributed to the trap states in GO [22]. In contrast to considerable transient absorption/transmission measurements [26–31] on graphene, detailed studies of transient absorption properties of GO are still limited [22, 23, 25] and the corresponding interpretation is also diverse. Particularly, the broadband transient spectra and

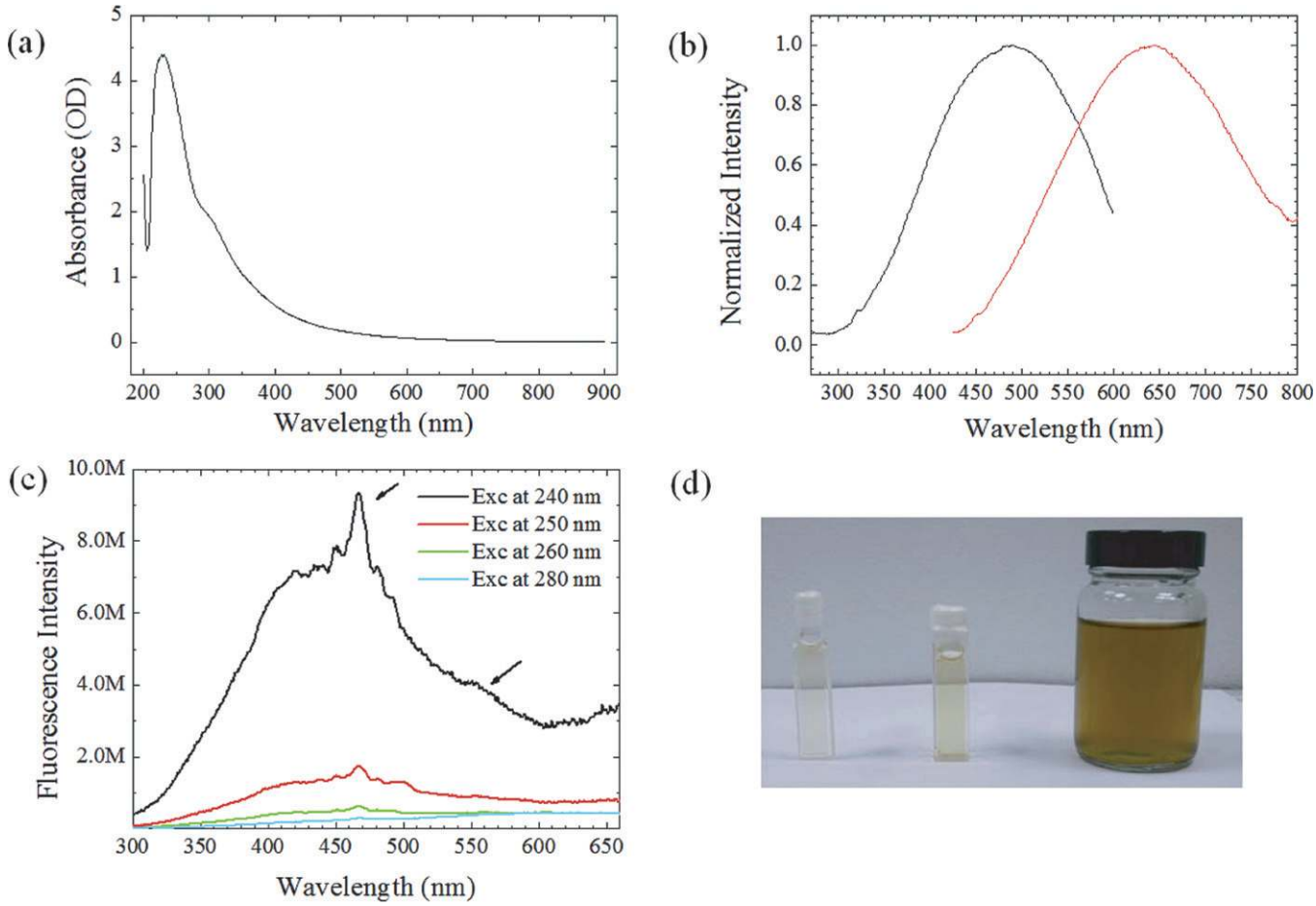

Figure 1. (*a*) Absorption spectrum of aqueous GO in a 2 mm cuvette; (*b*) fluorescence excitation and emission spectra of aqueous GO in a 10 mm cuvette at $\lambda_{em} = 640$ nm and $\lambda_{ex} = 410$ nm, respectively; (*c*) fluorescence emission spectra at excitation wavelengths of 240, 250, 260 and 280 nm; (*d*) photograph of the GO samples used.

wavelength-dependent kinetics of GO are rarely reported [22]. Moreover, the absorption-related electronic transitions in the broad visible range are still under discussion.

In this work, we focus on transient absorption properties of GO studied by femtosecond visible pump/white-light probe spectroscopy. The transient absorption spectra and kinetics have been determined over a broad probe region: both positive and negative absorbance changes were observed. Two-quantum absorption has been found at high excitation powers, which is reflected in the evolution of kinetic decay. Higher excited states emission, delayed rise of transient absorption and wavelength-dependent kinetics were studied. The absorption-related electronic transitions responsible for photobleaching, excited state absorption and stimulated emission processes have been discussed in detail.

2. Experiment details

The graphite oxide powders were prepared based on a modified Hummer's method [32–34]. The aqueous GO with a concentration of 0.5 mg ml^{-1} was obtained by ultrasonic treatment of graphite oxide powders in water and put into quartz cuvettes. In the sample, the C : O ratio is about 2.4 and three functional groups are C-O, C=O and O=C-OH with the relative ratio of 17 : 2 : 2 [19]. Steady-state absorption spectra were measured by a UV-Vis spectrophotometer (Cary 100 Bio, Varian). A spectrofluorometer (Fluorolog-3, HORIBA Jobin Yvon) was used to detect the fluorescence excitation and emission spectra. Transient absorption measurements were carried out by a femtosecond pump–probe system (Coherent, Legend Elite), which was described in the previous publications [35, 36]. The wavelength of pump pulses was centred at 480 nm and the probe beam was the white-light continuum generated by 800 nm pulses passing a CaF_2 plate. The pump beam was focused on 100 μm area on the sample.

3. Results and discussion

Figure 1 shows the steady-state absorption, fluorescence excitation and emission spectra, and the photograph of aqueous GO samples. Figure 1(*a*) presents the absorption spectrum of GO in the UV to near infrared range. The main peak and its shoulder are located at ~230 nm and ~300 nm, corresponding, respectively, to π–π^* and n–π^* transitions in carbon based materials [13, 21]. After 300 nm, the absorbance of GO gradually decreases. These absorption features are typical for as-prepared aqueous GO [3]. As shown in figure 1(*b*), the fluorescence excitation and emission spectra

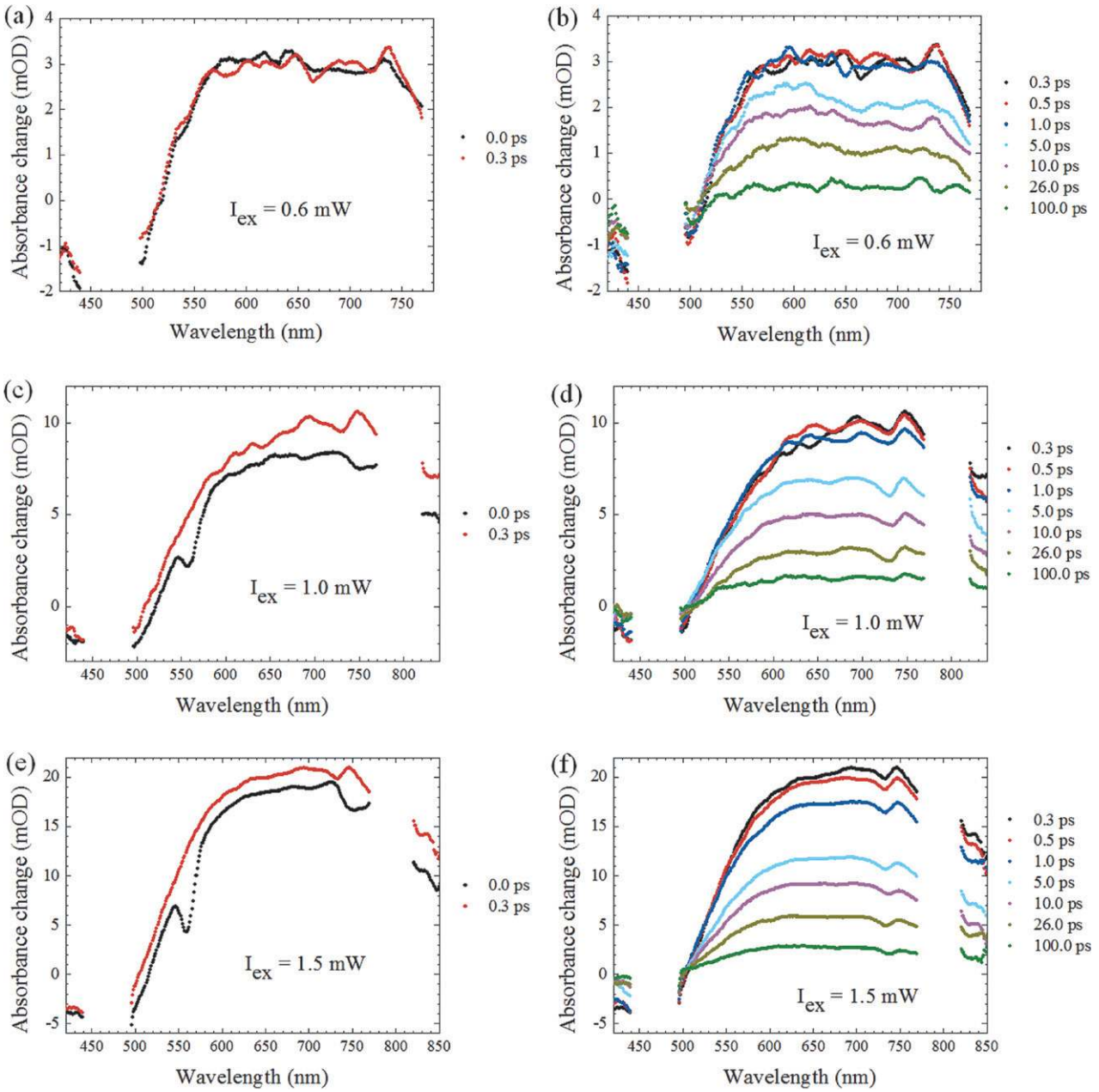

Figure 2. (*a*), (*b*) Transient absorption spectra of aqueous GO in a 2 mm cuvette at $I_{ex} = 0.6$ mW; (*c*), (*d*) transient absorption spectra of aqueous GO at $I_{ex} = 1.0$ mW; (*e*), (*f*) transient absorption spectra of aqueous GO in a 2 mm cuvette at $I_{ex} = 1.5$ mW. The pump wavelength is 480 nm.

were recorded at the emission wavelength $\lambda_{em} = 640$ nm and the excitation wavelength $\lambda_{ex} = 410$ nm, respectively. Note that the fluorescence excitation spectrum does not match with the absorption spectrum. At $\lambda_{ex} = 410$ nm, the wide fluorescence emission is found between 500 and 800 nm. Similarly, the broad spectral region of fluorescence excitation signals between 350 and 600 nm contributes to the emission of 640 nm. Moreover, with $\lambda_{ex} = 240$–280 nm, another fluorescence emission band is found between 300 and 600 nm (figure 1(*c*)). Particularly, at $\lambda_{ex} = 240$ nm, a narrow peak and a broad peak are found at ~467 and ~560 nm, respectively (indicated with arrows). Similar structured emission spectral features have also been observed in the GO suspensions under various pH environments [37], where the quasi-molecular structure in GO, i.e. COOH-connected sp2 domains, has been considered.

Figure 2 shows the transient spectra of aqueous GO at three excitation powers (I_{ex}) of 0.6, 1.0 and 1.5 mW. The probe wavelength regions $\lambda_{pr} = 440$–495 and 770–820 nm, i.e. where the scattered excitation beam caused large noise, are deleted. For higher excitation powers (1.0 and 1.5 mW), the spectral dips around 560 nm are caused by the stimulated Raman scattering of water under the 480 nm excitation (figures 2(*c*) and (*e*)). In the early 0.3 ps, the induced absorption and transmission were found at $\lambda_{pr} > 500$ nm and 420 nm $< \lambda_{pr} <$ 500 nm, respectively. It indicates that the excited state absorption is dominant at the spectral range of $\lambda_{pr} > 500$ nm, and photobleaching is dominant at λ_{pr}

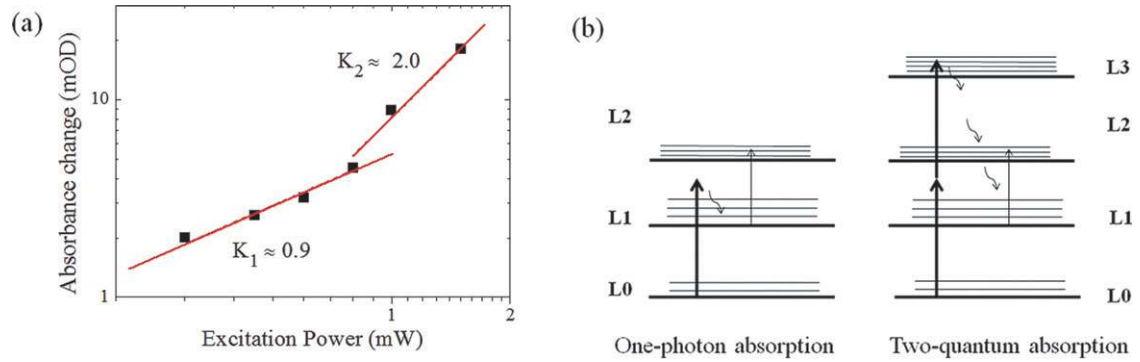

Figure 3. (*a*) Excitation power dependence of the absorbance change at $\lambda_{pr} = 600$ nm. (*b*) Schematic of one-photon and two-quantum absorption; the pump and the probe photons as denoted by thick and thin arrows, respectively.

between 420 and 500 nm. During this stage, the initial induced absorption amplitudes remain for $I_{ex} = 0.6$ mW (figure 2(*a*)) while they increase for $I_{ex} = 1.0$ and 1.5 mW (figures 2(*c*) and (*e*)), which is related to two-quantum absorption discussed later. Note that the delayed rise of the transient absorption is observed in GO for the first time. With the increase of I_{ex}, both absorption and photobleaching features become more apparent. After 0.3 ps, the transient spectra are shown in figures 2(*b*), (*d*) and (*f*). On the whole, the spectral amplitudes, indicating the electron population, decrease with the decay time, which indicates the relaxation of excited electrons. Besides, the spectral features around 730 nm as shown in figures 2(*d*) and (*f*) are related to the absorption of water as discussed previously [19].

Figure 3(*a*) shows the excitation power dependence of absorbance change (ΔA) of GO at the probe wavelength of 600 nm. For low excitation powers (0.3–0.8 mW), the slope is 0.9, which is indicative of linear process. At higher excitation powers (1.0 and 1.5 mW) the slope is 2, i.e. dependence is quadratic. In contrast to the classical two-photon absorption for transparent materials, the observed behaviour we call two-quantum absorption in view of the existence of absorption band in the detected spectral region. In this case we have a consecutive (stepwise) absorption of two laser quanta via intermediate electronic state. For the observed increase of ΔA in the initial 0.3 ps (figures 2(*c*) and (*e*)), i.e. the delayed ΔA maximum, is due to the relaxation of excited electrons from upper excited states (e.g. L3) to the lowest excited states (L1). As shown in figure 3(*b*), in general, when electrons are excited from L0 to L1 by one-quantum absorption, the excited state (L1) absorption occurs from L1 to upper excited states; when electrons are excited from L0 to L3 by two-quantum absorption, the excited state (L1) absorption happens when the excited electrons relaxed from L3 to L1 via various decay processes. Therefore, the delayed rise of ΔA within 0.3 ps is a result of superposition of photobleaching (due to depletion of L1) and population of L1 due to relaxation from upper excited states (e.g. L2, L3), which is delayed in time. It is noted that nonlinear optical responses have been reported in GO [23, 25], such as saturable and two-photon absorption. Particularly, the two-photon absorption has been claimed to occur in sp3 domains in GO [23]. The large two-photon absorption coefficient of bilayer graphene measured by Z-scan technique has also been discussed according to a quantum perturbation theory [38].

Figures 4(*a*)–(*c*) show ΔA as a function of delay time at the probe wavelength of 640 nm with three excitation powers: 0.6, 1.0 and 1.5 mW. The decay curves are fit by a multi-exponential decay function convoluted with the instrument response function [36]. In all cases amplitudes are positive, which indicates that the predominant process is excited state absorption. With the increase of I_{ex}, the drop of amplitudes in the first 5 ps becomes more obvious. Global fit of decay curves at $\lambda_{pr} = 560$–720 nm and at $I_{ex} = 0.6$ mW results in three time components: $\tau_1 = 9.3$ ps, $\tau_2 = 92$ ps and $\tau_3 = 1523$ ps. At $I_{ex} = 1.0$ mW, the decay curves between 530 and 610 nm can be globally fit by the triexponential function with time constants of 13, 90 and 2000 ps while four time constants ($\tau_0 = 2.1$ ps, $\tau_1 = 13$ ps, $\tau_2 = 90$ ps and $\tau_3 = 2000$ ps) are required to well reproduce the kinetic curves between 620 and 770 nm. At $I_{ex} = 1.5$ mW, four time components are necessary to fit the decay curves between 590 and 710 nm. Moreover, the kinetic curve at 444 nm is shown in figure 4(*d*), where the negative amplitude decays with three time components: $\tau_0 = 2.1$ ps, $\tau_1 = 13$ ps and $\tau_2 = 90$ ps. Previously, the multi-exponential fluorescence decay behaviour of GO [18, 19] and oxygen plasma-treated graphene [39] have been reported, where the multiple emission excited states in GO are taken into account. In our case, the fast three time components (τ_0–τ_2) are assigned to the electron lifetimes in upper excited states and the longest component reflects the lifetime in the lowest excited state. Figure 4(*e*) shows a monoexponential decay of the negative amplitude at $\lambda_{pr} = 500$ nm: $\tau = 0.5$ ps. The negative transient absorption signals at $\lambda_{pr} = 444$ and 500 nm are most probably due to the photobleaching, because it correlates well with the position of fluorescence excitation spectrum (figure 1(*b*)). However, the possibility for stimulated emission, in particular, at high excitation intensities, cannot be fully ruled out: fluorescence emission spectrum (figure 1(*c*)) overlaps well with our negative transient wavelength range.

Figure 5 presents the fractional amplitudes of time components at three excitation powers. Versus the excitation power, the number of time components and their fractional amplitudes vary gradually. As shown in figure 5(*a*), at $I_{ex} = 0.6$ mW, the contribution of τ_1 at longer wavelengths slightly increases while that of τ_3 decreases, and contributions

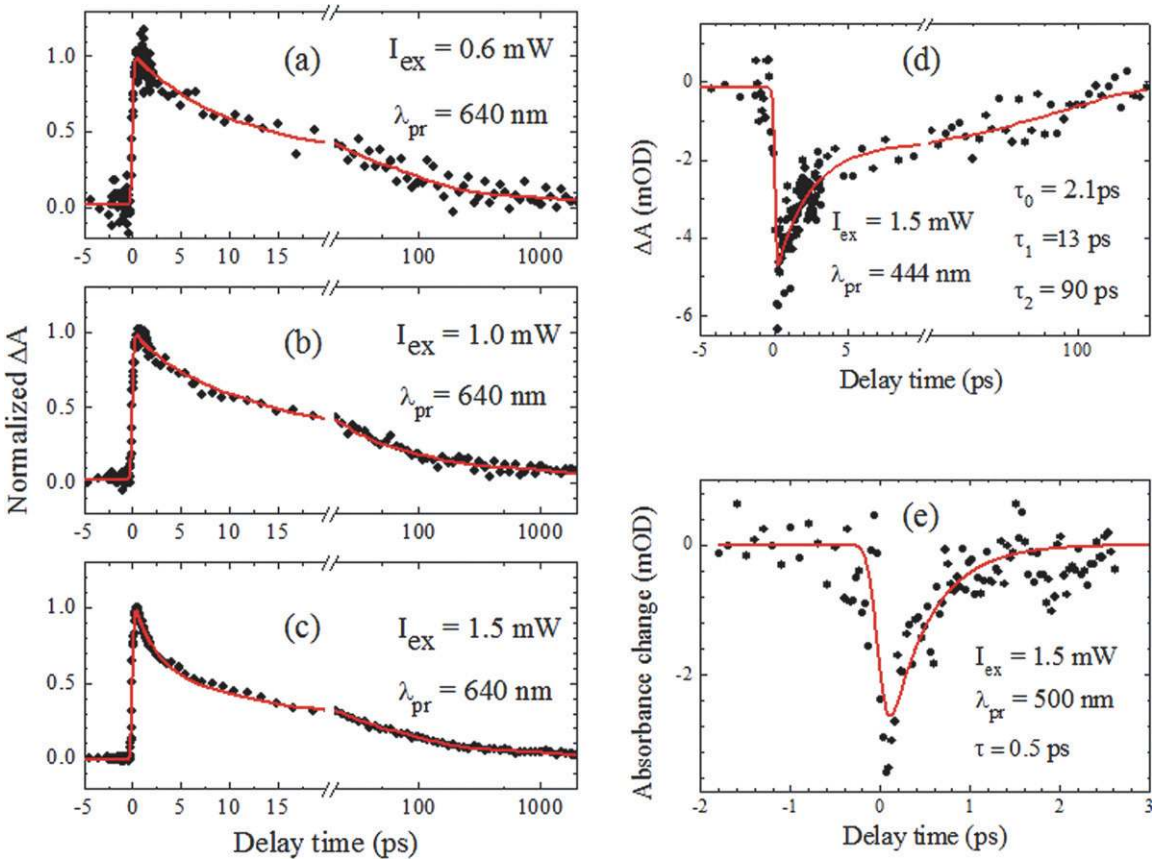

Figure 4. (*a*)–(*c*) Kinetic curves of GO in water at $\lambda_{pr} = 640$ nm under three excitation powers; (*d*) and (*e*) kinetic curves under 1.5 mW excitation at $\lambda_{pr} = 444$ nm and 500 nm, respectively.

of the shorter components (τ_1 and τ_2) are predominant. At $I_{ex} = 1.0$ mW, there are two spectral regions: 530–610 and 620–770 nm (figure 5(*b*)). The behaviour in the former region is similar to that at $I_{ex} = 0.6$ mW. However, at $\lambda_{pr} > 620$ nm, the competition of two shortest components is found: the new shortest component (τ_0) starts to become more important with the increase of λ and the contribution of τ_1 decreases. Meanwhile, the fractional amplitudes of two other components (τ_2 and τ_3) are invariant. At the high excitation power of 1.5 mW, the contribution of four components does not depend on λ_{pr} (figure 5(*c*)).

Figure 6 presents the quasi-molecular orbital energy levels and the electronic transitions in GO. The calculation details have been described elsewhere [19]. The electronic structure of GO can be considered as a dual gap system, which includes a narrow gap (between LUMO and HOMO) from sp2 regions and a wide gap (between L + 1 and H − 1) from sp2–sp3 hybrid regions. Localized states exist within the gaps (as denoted by dashed lines); these are caused by the nature of disorder structures of GO. At the low excitation power (e.g. $I = 0.6$ mW), one-photon absorption occurs (transitions 1 and 2 in figure 6). In the spectral range from 550 to 750 nm, the excited state absorption (transitions 5 and 6) is dominant rather than the photobleaching (transitions 7 and 8). The observed time components of (τ_1 and τ_2) are attributed to the absorption of localized states, which are related to fluorophore structures that consist of aromatic and oxidation groups in GO [19, 37]. The steady-state emission at $\lambda_{ex} = 410$ nm (figure 1(*b*)), is predominately from the transitions between L + 1 and H − 1. The time component of τ_3 is assigned to the transitions from LUMO to upper localized and excited states. At the high excitation power (e.g. $I = 1.5$ mW), two-quantum absorption may occur, represented as transitions 3 and 4. The absorption of excited states is dominant in the spectral range from 550 to 840 nm (figure 2), where the transitions can be from the states between LUMO and L + 1 to upper excited states (e.g. transitions 9 and 10). Meanwhile, the photobleaching (transitions 11 and 13) or stimulated emission (transitions 12 and 14) from 420 to 500 nm (figure 2(*e*)) and the steady-state fluorescence emission between 400 and 500 nm overlaps (figure 1(*c*)), where the corresponding transitions with time constants of (τ_0–τ_2) are dominant between L + 1 with upper localized states and H − 1 with lower localized states (e.g. transitions 11 and 12). Particularly, the observed peak 467 nm (figure 1(*c*)) is well consistent with the transition 12. Besides, upper excited states (>L + 1) can also contribute to the transient photobleaching (transition 13) and/or stimulated emission (transition 14) around 500 nm (figure 4(*e*)). In our previous time-resolved fluorescence measurements [19], we found five time components, where the short four components (1–500 ps) are assigned to the electronic states which are located higher than LUMO, and the longest one (~2 ns) is from LUMO. The present longest excited state absorption process is correlated to the longest emission time observed

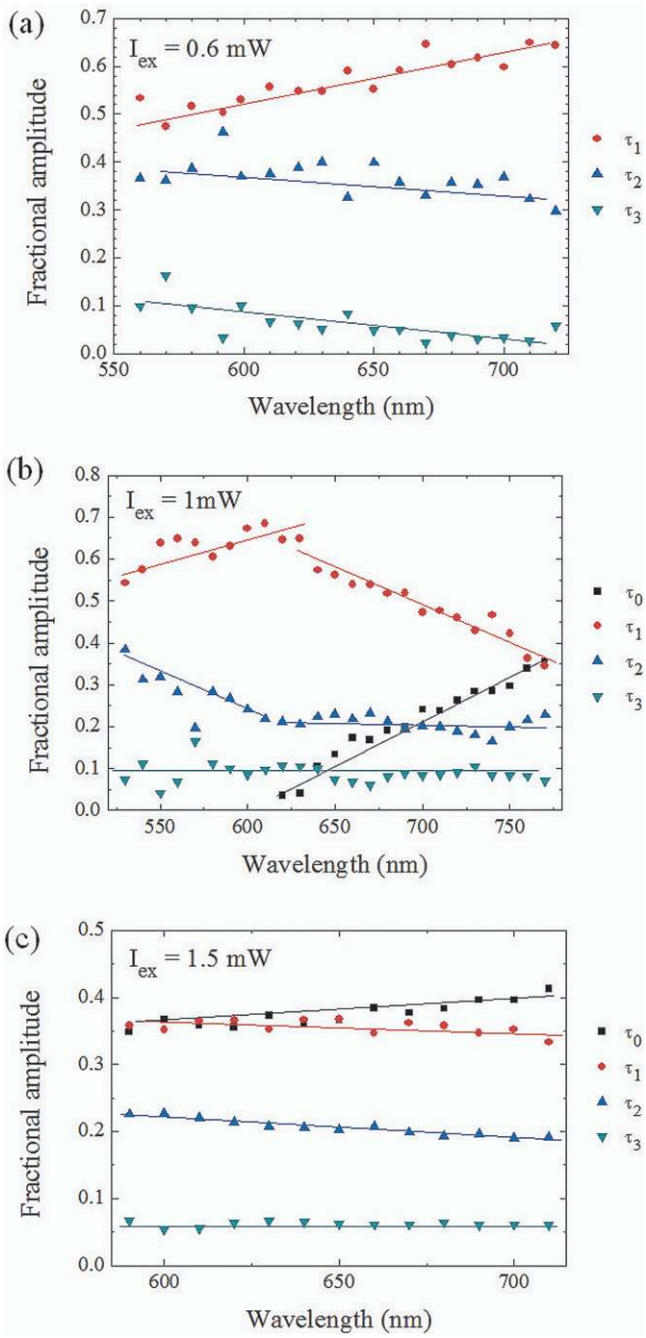

Figure 5. (*a*)–(*c*) Wavelength dependences of fractional amplitudes of time components at three excitation powers, respectively.

in [19]. Both processes reflect the same electronic lifetime at LUMO. The main reason for the deviation of the short components is that both transient absorption and fluorescence techniques are monitoring different transition processes even though they are probing the same states. In other words, time-resolved fluorescence reflects the transitions caused by emission while transient absorption signals result from the superposition of excited state absorption and photobleaching. Similar mismatch of time constants of transient absorption and time-resolved fluorescence data has also been reported in oxygen-plasma treated graphene samples by other groups [39]. Furthermore, our data show a long lifetime of 2 ns

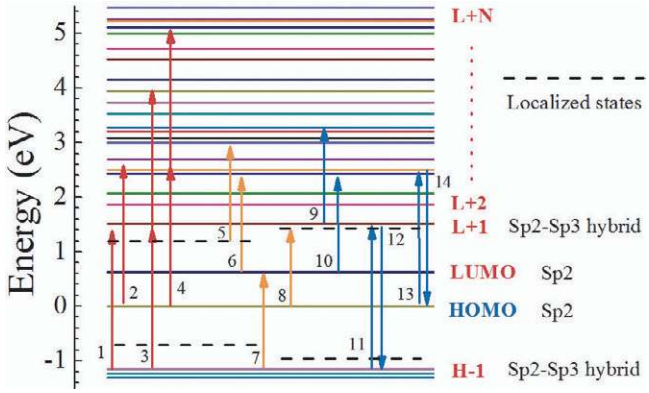

Figure 6. Quasi-molecular orbital energy levels (horizontal solid lines), representive localized states (dashed lines) and electronic trasitions (perpendicular lines with arrows) in GO.

unlike the previous transient transmission studies, where the longest time constant was 60–70 ps [23, 25]. Most probably, this discrepancy is caused by the oxidation degree of GO, the excitation conditions and the sample surrounding. For example, under the similar excitation conditions and the sample surrounding, a long lifetime in GO was found in [22] ($\tau > 400$ ps), which is consistent with our observations. However, the longest time we assign to the lowest excited states (LUMO) rather than the trap states (>400 ps) in [22]. The short three components (τ_0–τ_2) here are mainly from the excited states of sp2–sp3 hybrid regions and localized states rather than the decay process of carrier-optical phonon scattering in sp2 domains [25] and the excited states of sp3 domains [23]. Based on experimental data and theoretical calculations, absorption of different photon energies in GO has been assigned to the specified electronic transitions among the orbital energy levels and localized states, and the role of photobleaching, excited state absorption and stimulated emission was justified correspondingly.

4. Conclusion

Ultrafast pump–probe measurements have been carried out in order to study the electronic transitions in aqueous GO. Ultrafast carrier dynamics of excited states have been observed in the visible spectral range. The progression of transient absorption and kinetic decay were monitored with the increase of the excitation power. Delayed rise of differential absorption was found at higher excitation powers and was explained in terms of two-quantum absorption. The electron lifetimes in upper excited states and localized states of GO have been determined from both photobleaching/stimulated emission and excited state absorption kinetics. Finally, the electronic transitions under photoexcitation have been discussed based on the quasi-molecular orbital energy levels of GO.

Acknowledgments

We are grateful to Professor Maria-Elisabeth Michel-Beyerle for continuous support. Yu thanks the support of the Singapore National Research Foundation under NRF Award No NRF-RF2010-07.

References

[1] Dikin D A, Stankovich S, Zimney E J, Piner R D, Dommett G H B, Evmenenko G, Nguyen S T and Ruoff R S 2007 *Nature* **448** 457
[2] Dreyer D R, Park S, Bielawski C W and Ruoff R S 2010 *Chem. Soc. Rev.* **39** 228
[3] Eda G and Chhowalla M 2010 *Adv. Mater.* **22** 2392
[4] Eda G, Fanchini G and Chhowalla M 2008 *Nature Nanotechnol.* **3** 270
[5] Stoller M D, Park S J, Zhu Y W, An J H and Ruoff R S 2008 *Nano Lett.* **8** 3498
[6] Morales-Narvaez E and Merkoci A 2012 *Adv. Mater.* **24** 3298
[7] Loh K P, Bao Q L, Eda G and Chhowalla M 2010 *Nature Chem.* **2** 1015
[8] Ghosh T, Biswas C, Oh J, Arabale G, Hwang T, Luong N D, Jin M, Lee Y H and Nam J-D 2012 *Chem. Mater.* **24** 594
[9] Mao S, Pu H and Chen J 2012 *RSC Adv.* **2** 2643
[10] Kim J, Cote L J and Huang J 2012 *Acc. Chem. Res.* **45** 1356
[11] Sun X M, Liu Z, Welsher K, Robinson J T, Goodwin A, Zaric S and Dai H J 2008 *Nano Res.* **1** 203
[12] Luo Z T, Vora P M, Mele E J, Johnson A T C and Kikkawa J M 2009 *Appl. Phys. Lett.* **94** 111909
[13] Cuong T V, Pham V H, Tran Q T, Hahn S H, Chung J S, Shin E W and Kim E J 2010 *Mater. Lett.* **64** 399
[14] Shukla S and Saxena S 2011 *Appl. Phys. Lett.* **98** 073104
[15] Eda G, Lin Y Y, Mattevi C, Yamaguchi H, Chen H A, Chen I S, Chen C W and Chhowalla M 2010 *Adv. Mater.* **22** 505
[16] Subrahmanyam K S, Kumar P, Nag A and Rao C N R 2010 *Solid State Commun.* **150** 1774
[17] Xin G, Meng Y, Ma Y, Ho D, Kim N, Cho S M and Chae H 2012 *Mater. Lett.* **74** 71
[18] Chien C T *et al* 2012 *Angew. Chem. Int. Edn Engl.* **51** 6662
[19] Shang J Z, Ma L, Li J W, Ai W, Yu T and Gurzadyan G G 2012 *Sci. Rep.* **2** 792
[20] Exarhos A L, Turk M E and Kikkawa J M 2013 *Nano Lett.* **13** 344
[21] Luo Z T, Lu Y, Somers L A and Johnson A T C 2009 *J. Am. Chem. Soc.* **131** 898
[22] Kaniyankandy S, Achary S N, Rawalekar S and Ghosh H N 2011 *J. Phys. Chem.* C **115** 19110
[23] Liu Z B, Zhao X, Zhang X L, Yan X Q, Wu Y P, Chen Y S and Tian J G 2011 *J. Phys. Chem. Lett.* **2** 1972
[24] Ruzicka B A, Werake L K, Zhao H, Wang S and Loh K P 2010 *Appl. Phys. Lett.* **96** 173106
[25] Zhao X, Liu Z B, Yan W B, Wu Y P, Zhang X L, Chen Y S and Tian J G 2011 *Appl. Phys. Lett.* **98** 121905
[26] Sun D, Wu Z K, Divin C, Li X B, Berger C, de Heer W A, First P N and Norris T B 2008 *Phys. Rev. Lett.* **101** 157402
[27] Dawlaty J M, Shivaraman S, Chandrashekhar M, Rana F and Spencer M G 2008 *Appl. Phys. Lett.* **92** 042116
[28] Newson R W, Dean J, Schmidt B and van Driel H M 2009 *Opt. Express* **17** 2326
[29] Huang L B, Hartland G V, Chu L Q, Luxmi, Feenstra R M, Lian C X, Tahy K and Xing H L 2010 *Nano Lett.* **10** 1308
[30] Winnerl S, Orlita M, Plochocka P, Kossacki P, Potemski M, Winzer T, Malic E, Knorr A, Sprinkle M, Berger C, de Heer W A, Schneider H and Helm M 2011 *Phys. Rev. Lett.* **107** 237401
[31] Shang J Z, Yan S X, Cong C X, Tan H S, Yu T and Gurzadyan G G 2012 *Opt. Mater. Express* **2** 1713
[32] Hummers W S and Offeman R E 1958 *J. Am. Chem. Soc.* **80** 1339
[33] Cote L J, Kim F and Huang J X 2009 *J. Am. Chem. Soc.* **131** 1043
[34] Zhou X F and Liu Z P 2010 *Chem. Commun.* **46** 2611
[35] Shang J, Yu T and Gurzadyan G G 2012 *Appl. Phys.* B **107** 131
[36] Shang J Z, Yu T, Lin J Y and Gurzadyan G G 2011 *ACS Nano* **5** 3278
[37] Galande C, Mohite A D, Naumov A V, Gao W, Ci L J, Ajayan A, Gao H, Srivastava A, Weisman R B and Ajayan P M 2011 *Sci. Rep.* **1** 85
[38] Yang H Z, Feng X B, Wang Q, Huang H, Chen W, Wee A T S and Ji W 2011 *Nano Lett.* **11** 2622
[39] Gokus T, Nair R R, Bonetti A, Bohmler M, Lombardo A, Novoselov K S, Geim A K, Ferrari A C and Hartschuh A 2009 *ACS Nano* **3** 3963